2019

Effect of calcination temperature on the photocatalytic activity of carbon-doped titanium dioxide revealed by photoluminescence study

Nor Arbani Sean, *University Technology Malaysia*
Wai Loon Leaw, *University Technology Malaysia*
Hadi Nur, *University Technology Malaysia*

Received: 18 October 2018 | Revised: 10 January 2019 | Accepted: 28 January 2019

DOI: 10.1002/jccs.201800389

JOURNAL OF THE CHINESE CHEMICAL SOCIETY

ARTICLE

Effect of calcination temperature on the photocatalytic activity of carbon-doped titanium dioxide revealed by photoluminescence study

Nor Arbani Sean[1] | Wai Loon Leaw[1] | Hadi Nur[1,2]

[1]Centre for Sustainable Nanomaterials, Ibnu Sina Institute for Scientific and Industrial Research, Universiti Teknologi Malaysia, UTM Skudai, Johor, Malaysia

[2]Central Laboratory of Minerals and Advanced Materials, Faculty of Mathematics and Natural Science, State University of Malang, Malang, Indonesia

Correspondence
Hadi Nur, Centre for Sustainable Nanomaterials, Ibnu Sina Institute for Scientific and Industrial Research, Universiti Teknologi Malaysia, 81310, UTM Skudai, Johor, Malaysia.
Email: hadi@kimia.fs.utm.my

Funding information
FRGS, Grant/Award Number: Vot.130000.7809.4F626; LRG Sunder the Nanomite Programme, Grant/Award Number: Vot.130000.7340.4L825

Carbon-doped titania (C-TiO_2) nanoparticles were synthesized by the sol–gel method at different calcination temperatures (300–600°C) employing titanium tetraisopropoxide (TTIP) as the titanium source and polyoxyethylene sorbitan monooleate (Tween 80) as the carbon source. The physical properties of C-TiO_2 samples were characterized by X-ray diffraction (XRD) and scanning electron microscopy (SEM). The photocatalytic activities were checked through the photodegradation of phenolphthalein (PHP) under ultraviolet irradiation. The UV spectrum showed that the carbon doping extends the absorption range of TiO_2 to the visible region. However, the photocatalytic activity is affected by the electron–hole recombination phenomenon, as revealed by the photoluminescence (PL) study. According to the PL spectra, carbon doping reduces the edge-to-edge electron–hole recombination. Nevertheless, the number of defect sites is greatly influenced by the calcination temperature of C-TiO_2. C-TiO_2 that was calcined at 400°C showed the highest photodegradation percentage of PHP, which was mainly attributed to the synergic effect of the low direct edge-to-edge electron–hole recombination, high content of defect sites, and retention of active electrons on the surface hydroxyl group.

KEYWORDS
carbon-doped titania, electron–hole recombination, photoluminescence spectroscopy

1 | INTRODUCTION

In order to be an efficient photocatalyst, the catalyst should have high stability in extreme environments and be photoactive, photostable, and low cost.[1,2] Titanium dioxide (TiO_2) is a widely used semiconductor since it provides all the special characteristics mentioned above. TiO_2 is an effective photocatalyst for water and air purification. However, TiO_2 has a large bandgap of 3.2 eV, which requires activation by UV light. This limits its photocatalytic activity under solar energy or visible light, which is the most abundant in the electromagnetic spectrum. Besides, TiO_2 also allows fast electron–hole recombination, which decreases the efficiency of photocatalytic activity. Over the years, doping has been one of the methods used to improve the properties of or impose new properties on TiO_2.[3] For example, some dopants could narrow down the bandgap so that TiO_2 is able to absorb abundant photons in the visible range (λ = 380–750 nm).

Among those improved materials, carbon-doped TiO_2[4] was found to be photosensitive in the visible light. Numerous experiments have dealt with substitutional doping with carbon from a wide variety of carbon sources.[5–7] As a result, the photocatalytic activity generally varied with the carbon concentration or even with the synthesis method. Most studies primarily have reported the effects of carbon

doping on the microstructure and optical properties TiO_2. Unfortunately, a comprehensive explanation of the inconsistent photocatalytic performance is still lacking.

This paper focuses on the effects of carbon doping as well as the influence of the calcination temperature on the microstructure and photocatalytic activity. The discussion is focused on the aspects of charge carrier recombination, which is studied by photoluminescence (PL) spectroscopy. The PL signal originates from the radiative recombination of charge carriers and allows us to understand the behavior of these carriers giving direct information on the photocatalytic activity. Besides, the surface and bulk defects are revealed as well. This is important because surface and bulk defects play a critical role in the performance of photocatalysts as chemically active or charge-trapping sites.[8] The PL spectra presented here provide insight into the interplay between different defect states resulting from the different calcination temperatures on C-TiO_2. This study will contribute to the pursuit of better technology in photocatalytic materials under visible light irradiation.

2 | RESULTS AND DISCUSSION

2.1 | Characterization

All samples were characterized using X-ray diffraction (XRD). Figure 1 shows the wide-angle XRD patterns of the reference anatase and titania photocatalysts. It can be seen that the calcination temperature influences the crystallization and phase composition of TiO_2. C-TiO_2 that was calcined at 300°C for 3 hr showed no distinct pattern in the XRD, indicating the dominance of the amorphous phase. Higher calcination temperature led to partial crystallization, showing the prominent peaks of anatase. Besides, the rutile phase appeared when the calcination temperature reached 600°C, as indicated by the peak at $2\theta = 27.4°$. It shows that a partial

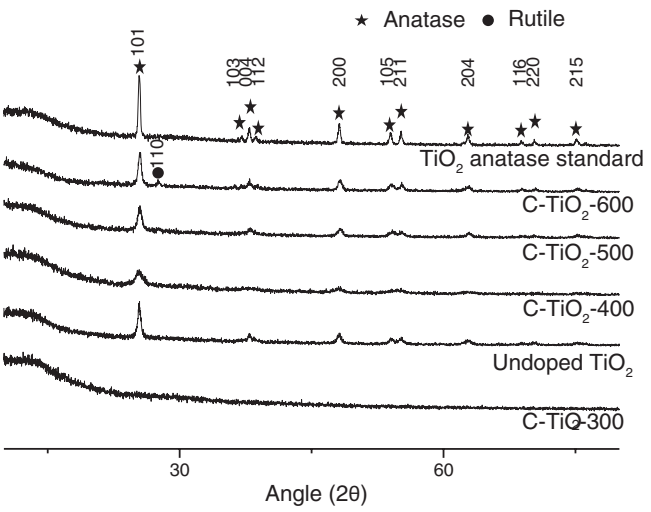

FIGURE 1 XRD patterns of TiO_2 anatase standard (Sigma Aldrich, 637254) and photocatalysts

transformation of the amorphous–anatase polymorph into amorphous–anatase–rutile phase mixture occurs. Referring to the peak (101), which is located at $2\theta = 25.4°$, the peak intensity increases and the width of the peak becomes narrower as the calcination temperature increases. Undoubtedly, the calcination temperature does have an effect on the particle size although the variation is very small. The increase in particle size is ascribed to thermally promoted crystalline growth.[9] According to Ratke and Voorhees, the crystalline growth is due to the growth of smaller anatase crystalline domains after nucleation through Ostwald ripening or through the combination of primary particles into larger secondary particles.[10] A previous study also reported that the increase in crystallite size is related to the growth of the crystal through agglomeration.[11] Most importantly, the effect of carbon on the TiO_2 particle size is confirmed. As compared to the undoped TiO_2 and C-TiO_2, both of which were calcined at the same temperature of 400°C, the intensity of the (101) plane diffraction peak of anatase TiO_2 decreased with carbon doping. The crystallite size of anatase was calculated based on the peak (101) using the Debye–Scherrer equation (Equation 1). In this equation, K is a dimensionless constant (taken as 0.89), λ is the wavelength of the characteristic X-ray applied (Cu Kα = 0.15406 nm), θ is half of the diffraction angle 2θ, and β is the full width at half-maximum height (FWHM) of the peak. As listed in Table 1, the crystallite size of TiO_2 decreases from 17 to 8 nm when TiO_2 is doped with carbon. The change in crystallite size is due to the presence of dissimilar boundaries created by carbon doping.[12]

$$D = (K\lambda/\beta \cos \theta). \quad (1)$$

The presence of carbon in TiO_2 was confirmed using Fourier transform infrared (FTIR) spectra. Figure 2 shows IR bands at 3,337, 2,162, 2,046, 1,979, 1,633 cm^{-1} and bands below 800 cm^{-1}. These bands are due to the vibrations of the different functional groups present. The C-TiO_2-400 spectrum shows a broad O–H stretching absorption centered around 3,337 cm^{-1} compared to the undoped TiO_2-400 spectrum. The broad shape is due to the O–H stretching of the adsorbed water molecules and the surface hydroxyl groups on the TiO_2 photocatalyst. The bands at 2,162, 2,046, and 1,979 cm^{-1} are the characteristics of the C=O

TABLE 1 Crystalline phase and size comparison between undoped TiO_2 and carbon-doped TiO_2 synthesized at different calcination temperature

Sample	Calcination temperature (°C)	Crystallite size (nm)	Anatase 85.6366 (%)	Rutile (%)
TiO_2-400	400	17	100	0
C-TiO_2-300	300	—	0	0
C-TiO_2-400	400	8	100	0
C-TiO_2-500	500	13	100	0
C-TiO_2-600	600	19	70	30

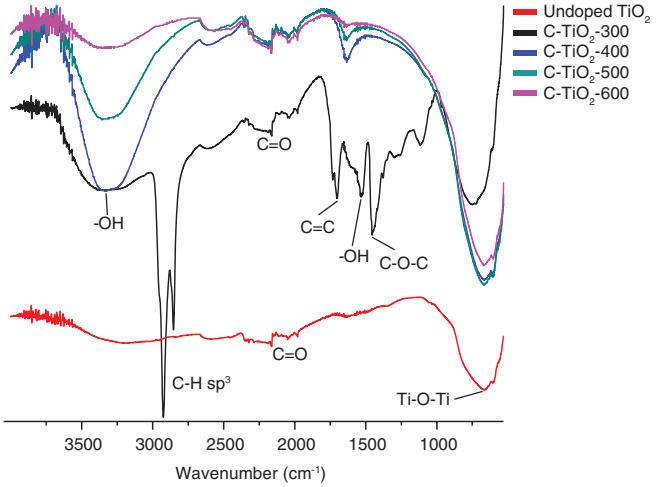

FIGURE 2 FTIR spectra of TiO_2 and carbon-doped TiO_2 photocatalysts

group from the surfactant. The band at 1,633 cm^{-1} is the characteristic peak of the chemisorbed O–H groups on the surface of TiO_2 nanoparticles. The bands below 800 cm^{-1} are attributed to Ti–O stretching and Ti–O–Ti bridging stretching modes.[13] As the temperature increases, the intensity of the O–H band centered at 3,337 cm^{-1} and the corresponding band at 1,633 cm^{-1} decrease in intensity. This indicates that the high calcination temperature resulted in a decrease in the number of hydroxyl groups present on the surface of the TiO_2 photocatalysts. The band appearing in the C-TiO_2-300 spectrum at 2,924 and 2,852 cm^{-1} are the characteristic peaks of C–H sp^3 asymmetric stretching and the symmetric stretch, respectively, from Tween 80. The bands at 1,699 and 1,456 cm^{-1} are attributed to the C=C and C–O–C vibrations, respectively. However, those bands disappear when the calcination temperature is increased, as they are converted into CO_2 at high temperatures. Besides that, the intensity of the Ti–O vibration band increases with the increase in the calcination temperature. This is because at a higher temperature, the rearrangement of Ti–O network and crystallization of TiO_2 are promoted.[14] The carbon content is also confirmed using scanning electron microscopy (SEM)-EDX (energy dispersive X-ray). As shown in Table 2, the carbon content reduces as the calcination temperature increases.

As revealed by SEM, the reference anatase TiO_2 powders have sperical shape and form sponge-like aggregates, wheras carbon-doped anatase and undoped anatase have uniformity in surface morphology and shape in the form of lamellar isolated aggregates. As shown in Figure 3, there are changes in the size of solid TiO_2, which is in correspondence with the XRD results. Before doping with carbon, the solid size is relatively large (Figure 3b) but after the addition of carbon, the particle size seems to decrease (Figure 3d). This implies that the addition of carbon dopants into TiO_2 reduces the growth of particle size. It can also be observed that the images shown at different calcination temperatures (Figure 3c–f) are irregular in shape. On increasing the calcination temperature, the particle size of the product increases and the particles show agglomeration.[15] The increase in particle size is in correspondence with the changes in the crystallite size, as mentioned before. This reveals that calcination temperature also affects the particle size of the synthesized C-TiO_2.

TABLE 2 SEM–EDX analysis of titania samples

	Element (wt%)		
Sample	**C**	**O**	**T**
C-TiO_2-300	63.0	23.2	13.8
C-TiO_2-400	11.7	39.6	48.7
C-TiO_2-500	7.30	30.3	62.4
C-TiO_2-600	4.20	38.9	56.9

2.2 | Photocatalytic activity

Figure 4 shows the photocatalytic degradation percentage of phenolphthalein (PHP). Undoped TiO_2-400 was active under UV light and was able to degrade PHP at 2.7×10^4 ppm. This is due to the large bandgap energy of TiO_2, which only be activated by the minute fraction of UV light in the solar photon flux.

Upon doping with carbon, the photodegradation of PHP varied with the calcination temperature. Among all the samples, C-TiO_2-300, C-TiO_2-500, and C-TiO_2-600 seem to have only a trace or even no photodegradation activity toward PHP. For C-TiO_2-300, the poor photocatalytic performance could be due to its amorphous phase indicated by XRD. As can be seen in the UV spectrum in Figure 5, C-TiO_2-300 actually has a wide adsorption throughout the UV and visible light. Besides, the bandgap as calculated via the Tauc model by plotting $(FRxhv)^2$ as a function of the photon energy (hv) is around 3.6 eV, indicating that C-TiO_2-300 could be activated under irradiation. However, the low performance of C-TiO_2-300 can be understood as due to its amorphous phase, which leads to high electron–hole recombination. Amorphous C-TiO_2-300 contains many imperfections such as impurities, dangling bonds, or microvoids, which act as an electron–hole recombination centers.[16,17]

The bandgap energies and the band edge positions of the photocatalysts, which were estimated using the Mulliken electronegativity equation below, are listed in Table 3.[18] Comparing the undoped and carbon-doped TiO_2, which were both calcined at 400°C, carbon doping does affect the E_g of TiO_2. Besides, the influence of carbon doping on E_g is highly dependent on the calcination temperature. The observed shift of the absorption and difference in E_g for C-doped TiO_2 samples indicate that carbon doping is very effective in increasing the optical response of TiO_2 in the visible region. Carbon doping provides a new electronic state in the middle of the bandgap, where the charge-transfer transition occurs between the conduction band of the dopant and the conduction band of the TiO_2 itself. It has been

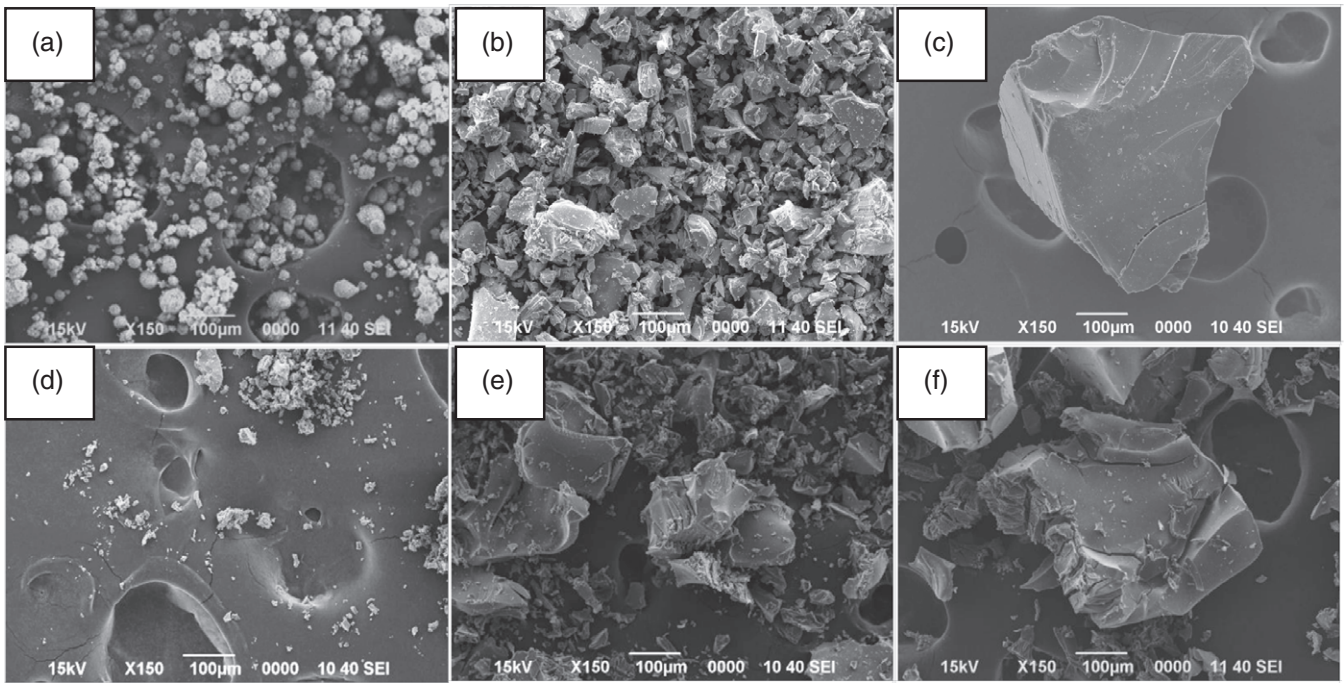

FIGURE 3 SEM micrographs of (a) TiO_2 anatase standard (Sigma Aldrich, 637254), as-prepared (b) undoped TiO_2, (c) C-TiO_2-300, (d) C-TiO_2-400, (e) C-TiO_2-500, and (f) C-TiO_2-600

reported that nonmetal elements could reduce the E_g of TiO_2 by mixing the p orbital of the nonmetal with the O 2p orbital and the doping of various transitional-metal ions into TiO_2 could shift its optical absorption edge from the UV to the visible region without any prominent change in the TiO_2 bandgap.[19] It was reported that at high calcination temperature, there are a few factors that contribute to the bandgap narrowing. First of all, it is due to the changes in the titania phase mix; for instance, at 600°C, the C-doped TiO_2 consist of 70% anatase and 30% rutile (Table 1). The increase in the rutile phase has significantly decreased the E_g values of the prepared samples. Second, due to the progressive development of oxygen vacancies (OVs), a large number of active sites are present in the samples under visible light.[20] Thus, it can be deduced that the presence of the OV states reduces E_g at higher calcination temperatures. In addition, it was reported that the decrease in E_g is also due to the efficient carbon doping in the TiO_2 lattice structure.[21] Previously, it was proven that carbon could absorb more visible light and improve the synergistic properties between TiO_2 and carbon by forming a joint electronic system.[22] Therefore, it was assumed that the bandgap of C-doped TiO_2 can be tuned by varying the calcination temperature.

$$E_{CB} = \chi - E_e - 0.5\,(E_g), \tag{2}$$

$$E_{VB} = E_{CB} - E_g, \tag{3}$$

where E_{CB} and E_{VB} are the conduction band edge and valence band edge, respectively, and χ is the Mulliken electronegativity (5.89 eV). E_e is the energy of the free electrons on the hydrogen scale (~4.5 eV), and E_g is the band gap energy of the prepared samples.[18]

Since all samples have bandgap energy that could be activated by UV light, it is curious that the crystalline phase

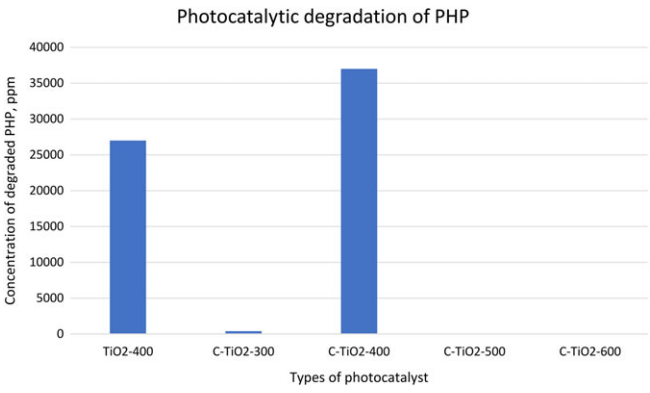

FIGURE 4 Photocatalytic degradation percentage of PHP in the presence of a different catalysts under UV light irradiation

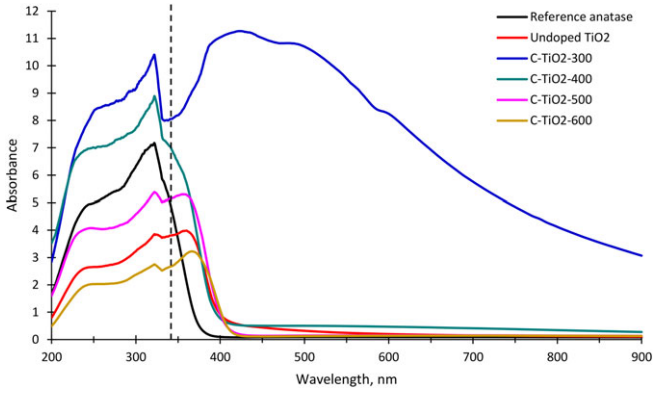

FIGURE 5 UV–vis diffuse reflectance spectra of reference anatase TiO_2, undoped TiO_2, and C-TiO_2 calcined at a different temperatures

TABLE 3 Bandgap energy, calculated conduction band, and valence band edge positions of the photocatalysts

Sample	E_g (eV)	E_{CB} (eV)	E_{VB} (eV)
Undoped TiO_2	3.16	−0.19	−3.35
C-TiO_2-300	3.60	−0.41	−4.01
C-TiO_2-400	3.24	−0.23	−3.47
C-TiO_2-500	3.16	−0.19	−3.35
C-TiO_2-600	3.08	−0.15	−3.23

is the main factor influencing the photocatalytic activity of TiO_2. Obviously, the lower bandgap energy does not improve the photocatalytic performance of C-TiO_2 because C-TiO_2-600, which has lowest bandgap energy, did not degrade PHP. Looking into the XRD data, C-TiO_2-500 and C-TiO_2-600, which possess the pure anatase phase and a mixture of anatase–rutile phase, respectively, did not degrade PHP. It can be assumed that the electron–hole activity is the key factor that determines the photocatalytic activity of C-TiO_2.

C-TiO_2-400 has the highest photodegradation toward PHP (3.7×10^4 ppm), even higher than that of undoped TiO_2 that was calcined at the same temperature. Considering their similar physical and optical properties, PL study was carried out to investigate the electron–hole activity of the photocatalyst. If we hypothesize that electron–hole activity is the key factor that determines the photocatalytic activity, the PL spectrum should show a distinct difference. PL spectroscopy is a good technique to understand the separation efficiency of photogenerated electrons and holes.[23] Figure 6 illustrates the PL spectra of undoped TiO_2 and C-TiO_2 samples calcined at 300, 400, 500, and 600°C in the range 340–600 nm under 325 nm excitation. It is seen that the three spectra exhibit almost similar type of curve shape and the positions of the peaks are nearly the same, demonstrating that carbon doping does not give rise to new PL phenomena. The UV emission peaks of undoped TiO_2 and C-TiO_2-400 at 345 nm are due to the electron transition from the minimum of the conduction band to the valence band, while those at 380, 400, and 406 nm are due to the self-trapped excitons (STEs).[24,25] It was reported that STE is the result of capturing holes by a trapped electron in the lattice site.[26] The energy level of the excitons is then lowered by impurity-assisted self-trapping, thus providing a low rate of recombination.[27] STE emission can occur through direct or indirect recombination of the carriers through OVs.[28] In this study, the STE emission is in the indirect mode since carbon doping generates OV.

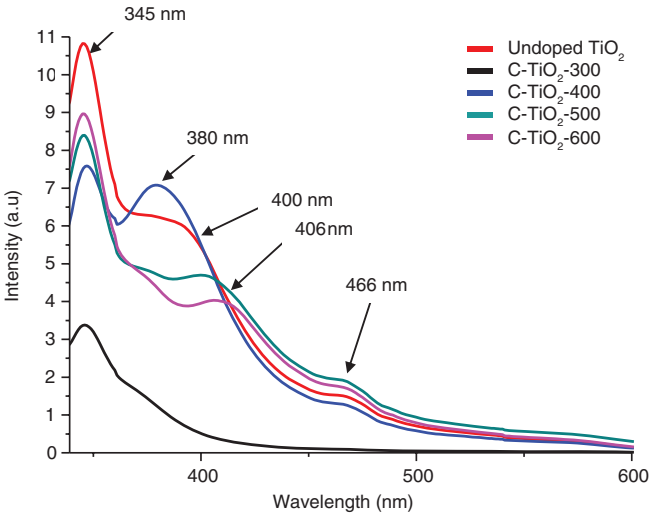

FIGURE 6 Photoluminescence spectra of TiO_2 and carbon-doped TiO_2 calcined at 300–600°C

Besides that, there is one more visible emission peak present in all the synthesized samples at 466 nm. According to Lei et al., this peak is related to the excitons and oxygen defect associated with shallow and deep trap centers called the F or F^{2+} center.[21,29] The site where two electrons are trapped in an OV is called the F center, while those with no trapped electron is called the F^{2+} center. Generally, PL spectra of anatase TiO_2 have different kinds of physical origins, which are STEs, OVs, and surface states. Some authors have reported that shallow traps identified as OVs are at 465 nm.[30] The 466 nm band in Figure 6 is associated with this trap. Therefore, the peak observed can be assigned to the OV states with different charges (F or F^{2+}). For an understanding of the effect of C doping at different calcination temperatures, the intensity of each band obtained in Figure 6 was analyzed. It was found that the presence of C quenches the peak intensity of each band. In general, some factors that could reduce the intensity of the emission peaks are structural defects, carrier mobility and trap centers, and nonradiative Auger-type recombination.[30] First of all, the decrease of the emission intensity of UV and STE peaks is due to structural defects, trap centers, and carrier mobility.[26,31] Structural defects are mainly related to grain boundary defects. The OVs generated via carbon doping will migrate to the grain boundaries and increase the number of oxygen defects. It was reported that XRD peaks are closely related with grain boundary defects.[30] From the XRD obtained in Figure 1, it can be found that the broad diffraction peaks with the smallest size of nanocrystalline materials provide the highest number of grain boundary defects. In contrast, the sharp and narrow diffraction peaks with large nanocrystalline materials have the smallest structural defects. Thus, it can be understood that carbon doping will increase the structural defects, resulting in low PL spectra intensity. Moreover, as mentioned, the defects created by carbon doping are certainly associated with the formation of F and F^{2+} trap centers. That charged site of OV will delay the recombination rate of e^- and h^+ since it will repel the mobile carrier that migrates through the lattice site. The increase in carbon doping will slow down the mobility of the free electrons to recombine with the holes inside or on the surface of the nanoparticles and, most importantly, will quench the emission intensity.[30] Apart from structural defects, the most

crucial factor that affects the reduction in emission intensity peaks is Auger-type recombination phenomenon. According to Wang et al., this process depends on the number of dopants and defects in the lattice.[32] Since doping introduces additional free electrons in the lattice of TiO_2, these free electrons will produce a nonradiative channel called Auger-like recombination channel and decrease the emission efficiency. The process involves the absorption of energy released through the recombination by one electron by another to be dissipated as phonons, thus quenching the intensity of the UV emission peaks. Furthermore, it was reported that the interaction of the excitons with lattice defects and dopants also reduces the peak intensity by the collapse the STE to free electron.[26]

Besides effective electron–hole separation, the retention of the excited electron on the surface of photocatalyst seems to be crucial as well. As shown by the UV spectrum, C-TiO_2-400 has the highest OH content compared to the others. The decrease in the number of hydroxyl groups on the surface of TiO_2 seems to be correlated with the photocatalytic activity. It is well known that the surface hydroxyl groups can promote the formation of a large number of •OH radicals to oxidize the organic pollutants, thus inhibiting the recombination of photogenerated charges and holes.[33] This is because the presence of OH offers more reaction sites for the oxidation of water molecules and production of hydroxyl radicals, thus enhancing the photocatalytic efficiency of the photocatalysts toward PHP.[34] It can be seen that the degradation percentage of photocatalyst is the order C-TiO_2-400 (11.9%) > C-TiO_2-500 (1.9%) > C-TiO_2-300, C-TiO_2-600, and undoped TiO_2 (0% each). The trend of the photocatalytic activity is not only caused by the crystalline phase, crystallite size, and particle size but also by the formation of defect sites and the different rates of electron–hole recombination

3 | EXPERIMENTAL

3.1 | Materials

TiO_2 anatase standard (Sigma Aldrich, 637254), titanium (IV) isopropoxide (97%, Aldrich) polyoxyethylene sorbitan monooleate (Vetec), acetic acid (99.8%, Bendosen), 2-propanol (99.8%, Emsure), PHP (99.81%, Emory) were used without any further purification. Deionized water was used throughout the experiments.

3.2 | Methodology

The synthesis was conducted according to Cai et al.[19] Five milliliters of Tween 80 was dissolved in 20 mL of isopropyl alcohol (i-PrOH) followed by the addition of 3 mL of acetic acid. Then, 3 mL of titanium tetraisopropoxide (TTIP) was added under vigorous stirring for 1 hr. The prepared sol–gel was aged at 65°C for 24 hr. Finally, the sol was dried for 3 hr at room temperature and then calcined in air at 300, 400, 500, and 600°C for 3 hr. Undoped TiO_2 was prepared by the same method without adding the corresponding dopant. The catalyst samples produced were denoted as undoped TiO_2, C-TiO_2-300, C-TiO_2-400, C-TiO_2-500, and C-TiO_2-600.

3.3 | Characterization

Samples were characterized using a Nicolet 6700 Thermo Scientific infrared spectrophotometer in the attenuated total reflection (ATR) mode. For UV–vis spectroscopy, a Perkin Elmer Lambda 900 spectrometer was used. The surface morphology of the samples was analyzed using SEM at an acceleration voltage of 15 kV. The phase and the crystallite size of the TiO_2 were determined by using an X-ray diffractometer (Bruker AXS D8 Automatic Powder Diffractometer). Anatase/rutile percentages were calculated from the resulting diffractograms using the Spurr equation (Equation 4)[35]:

$$\%_{\text{Rutile}} = 1/[1 + 0.8(I_{\text{Anatase}}(101)/I_{\text{Rutile}}(110)], \quad (4)$$

where I_{Anatase} is the intensity of the anatase peak from the (101) plane, and I_{Rutile} is the intensity of rutile peak from the (110) plane.[35] The PL spectra were measured at room temperature using a JASCO spectrofluorometer (FP-8500) with a Xe lamp as the excitation source (λ_{EX} = 325 nm, λ_{EM} = 340–600 nm).

3.4 | Photocatalytic activity

All photocatalytic degradation experiments were conducted in a self-built photocatalytic reactor, which was placed in a dark box to avoid the loss of UV. A 15 W lamp from Vilber Lourmat with maximum intensity at 254 nm was used as UV light source. The degradation percentage for each sample was calculated using Equation 5:

$$D\ (\%) = ([C_o - C]/C_o) \times 100 \quad (5)$$

where C_o is the initial concentration of PHP, and C is the concentration of PHP after treating with UV light radiation, in concentration unit (mg/L). About 50 mL of 10 ppm stock solution of PHP and 0.02 g of undoped TiO_2 were taken in a 100-mL beaker. The solution mixture was placed inside the prepared box and stirred using a magnetic stirrer. The system was stirred continuously in the dark for 1 hr, and about 3 mL of the solution was taken every 30 min for analysis. Then, the UV lamp was switched on. An aliquot of 3 mL was collected each hour for about 5 hr. The absorption of each sample was analyzed using the UV–vis spectrophotometer. The same method of preparation was used for all photocatalysts.

4 | CONCLUSIONS

Carbon-doped TiO_2 nanoparticles were successfully synthesized via the sol–gel route. The photocatalysts were calcined

at a different temperature of 300, 400, 500, and 600°C for 3 hr. C-TiO_2 photocatalyst calcined at 400°C was found to be most effective with an optimum number of carbons, hydroxyl group, and the existence of subband, which reduced the E_g values of the photocatalysts. Thus, it exhibited high degradation percentage of PHP under UV light irradiations, leading to as much as 3.7×10^4 ppm. It can be concluded that carbon doping is effective in creating defects that inhibit the electron–hole recombination. Besides, the OH groups on the surface can further retain the activated electrons for further reaction.

ACKNOWLEDGMENTS

This work supported by the LRGS grant Vot.130000. 7340.4L825 under the Nanomite Programme and the FRGS grant Vot.130000.7809.4F626.

ORCID

Hadi Nur https://orcid.org/0000-0002-4387-431X

REFERENCES

[1] A. Mills, R. H. Davies, D. Worsley, *Chem. Soc. Rev.* **1993**, *22*, 417.
[2] M. Pelaez, N. T. Nolan, S. C. Pillai, M. K. Seery, P. Falaras, A. G. Kontos, P. S. Dunlop, J. W. Hamilton, J. A. Byrne, K. O'shea, *Appl. Catal., B* **2012**, *125*, 331.
[3] A. Syafiuddin, T. Hadibarata, N. F. Zon, *J. Chin. Chem. Soc.* **2017**, *64*, 1333.
[4] J. Buha, *Thin Solid Films* **2013**, *545*, 234.
[5] H. Wang, J. P. Lewis, *J. Phys.: Condens. Matter.* **2005**, *17*, L209.
[6] H. Irie, Y. Watanabe, K. Hashimoto, *Chem. Lett.* **2003**, *32*, 772.
[7] W. Ren, Z. Ai, F. Jia, L. Zhang, X. Fan, Z. Zou, *Appl. Catal., B* **2007**, *69*, 138.
[8] A. L. Linsebigler, G. Lu, J. T. Yates Jr.. , *Chem. Rev.* **1995**, *95*, 735.
[9] S. Mahshid, M. Askari, M. S. Ghamsari, *J. Mater. Process. Technol.* **2007**, *189*, 296.
[10] L. Ratke, P. W. Voorhees, *Growth and Coarsening: Ostwald Ripening in Material Processing*, Springer Science & Business Media, Berlin **2013**.
[11] A. Gaber, M. Abdel-Rahim, A. Abdel-Latief, M. N. Abdel-Salam, *Int. J. Electrochem. Sci.* **2014**, *9*, 81.
[12] R. Rajkumar, N. Singh, *J. Nanomed. Nanotechnol.* **2015**, *6*, 1.
[13] A. M. Peiró, J. Peral, C. Domingo, X. Domènech, J. A. Ayllón, *Chem. Mater.* **2001**, *13*, 2567.
[14] J.-G. Yu, H.-G. Yu, B. Cheng, X.-J. Zhao, J. C. Yu, W.-K. Ho, *J. Phys. Chem. B* **2003**, *107*, 13871.
[15] A. B. Lavand, Y. S. Malghe, *Adv. Mater. Lett.* **2015**, *6*, 695.
[16] B. Ohtani, Y. Ogawa, S.-i. Nishimoto, *J. Phys. Chem. B* **1997**, *101*, 3746.
[17] G. Liu, C. Han, M. Pelaez, D. Zhu, S. Liao, V. Likodimos, N. Ioannidis, A. G. Kontos, P. Falaras, P. S. Dunlop, *Nanotechnology* **2012**, *23*, 294003.
[18] P. Reunchan, A. Boonchun, N. Umezawa, *Phys. Chem. Chem. Phys.* **2016**, *18*, 23407.
[19] J. Cai, W. Xin, G. Liu, D. Lin, D. Zhu, *Mat. Res.* **2016**, *19*, 401.
[20] H. Albetran, B. O'Connor, I. Low, *Mater. Des.* **2016**, *92*, 480.
[21] X. Wu, S. Yin, Q. Dong, C. Guo, H. Li, T. Kimura, T. Sato, *Appl. Catal., B* **2013**, *142*, 450.
[22] P. Zhang, C. Shao, Z. Zhang, M. Zhang, J. Mu, Z. Guo, Y. Liu, *Nanoscale* **2011**, *3*, 2943.
[23] W. Raza, M. Haque, M. Muneer, D. Bahnemann, *Arabian J. Chem.* **2015**. https://doi.org/10.1016/j.arabjc.2015.09.002.
[24] L. De Haart, A. De Vries, G. Blasse, *J. Solid State Chem.* **1985**, *59*, 291.
[25] N. Serpone, D. Lawless, R. Khairutdinov, *J. Phys. Chem.* **1995**, *99*, 16646.
[26] B. Choudhury, A. Choudhury, *J. Lumin.* **2013**, *136*, 339.
[27] M. Schreiber, Y. Toyozawa, *J. Phys. Soc. Jpn.* **1982**, *51*, 1544.
[28] K. Iijima, M. Goto, S. Enomoto, H. Kunugita, K. Ema, M. Tsukamoto, N. Ichikawa, H. Sakama, *J. Lumin.* **2008**, *128*, 911.
[29] Y. Lei, L. Zhang, G. Meng, G. Li, X. Zhang, C. Liang, W. Chen, S. Wang, *Appl. Phys. Lett.* **2001**, *78*, 1125.
[30] B. Choudhury, M. Dey, A. Choudhury, *Appl. Nanosci.* **2014**, *4*, 499.
[31] Y. Yamada, Y. Kanemitsu, *Appl. Phys. Lett.* **2012**, *101*, 133907.
[32] X. Wang, C. Song, K. Geng, F. Zeng, F. Pan, *Appl. Surf. Sci.* **2007**, *253*, 6905.
[33] M. A. Mohamed, W. N. W. Salleh, J. Jaafar, M. S. Rosmi, Z. A. M. Hir, M. A. Mutalib, A. F. Ismail, M. Tanemura, *Appl. Surf. Sci.* **2017**, *393*, 46.
[34] C. Xu, G. Rangaiah, X. Zhao, *Ind. Eng. Chem. Res.* **2014**, *53*, 14641.
[35] N. T. Nolan, M. K. Seery, S. C. Pillai, *J. Phys. Chem. C* **2009**, *113*, 16151.

How to cite this article: Sean NA, Leaw WL, Nur H. Effect of calcination temperature on the photocatalytic activity of carbon-doped titanium dioxide revealed by photoluminescence study. *J Chin Chem Soc*. 2019;1–7. https://doi.org/10.1002/jccs.201800389